Parity-Time Symmetry and its Applications in Optics

Rohith Chandrasekar
Physics 522: Quantum Optics
Final Paper

Parity-Time ($\mathcal{PT}$) symmetric quantum Hamiltonian systems have attracted great interest in the past few years, since the seminal discovery by Bender et al [1] in 1998 that these non-Hermitian Hamiltonians have real and positive eigenvalues. Since then, there have been numerous efforts to observe these phenomena experimentally, and it has been shown that optics may be the most suitable platform for this. In this paper, we aim to give an overview of $\mathcal{PT}$ symmetric Hamiltonian systems, from theory development to most recent applications in optics, specifically a coupled waveguide study by Ruter et al, and a microcavity study by Peng et al.

1. Theory Development

In 1998, Carl Bender et al published a paper on Non-Hermitian Hamiltonians exhibiting $\mathcal{PT}$ symmetry [1]. A Hamiltonian H is said to be $\mathcal{PT}$ if it obeys $\mathcal{PT}H = H\mathcal{PT}$, i.e. the Hamiltonian and the $\mathcal{PT}$ operator have the same eigenvectors. Their work was based off a conjecture made some years prior by D. Bessis. Bessis had conducted numerical studies on a unique non-Hermitian Hamiltonian having the form $H = p^2 + x^2 + ix^3$, discovering that it had all real and positive eigenvalues, a property exclusively attributed to Hermitian matrices.

Bender et al. took the conjecture further, claiming this Hamiltonian was in a class of matrices exhibiting Parity-Time symmetry. From standard Quantum Mechanical treatment, the parity operator makes spatial reflections by $\mathcal{P}: p \to -p, x \to -x$. Similarly, the time reversal operator replaces $\mathcal{T}: i \to -i$. Since $p = -i\frac{\partial}{\partial x}$, the time reversal operator also reflects $p \to -p$. We notice that when we apply each operator separately, the Hamiltonian is not conserved; $\mathcal{P}: H = p^2 + x^2 - ix^3$, $\mathcal{T}: H = p^2 + x^2 - ix^3$. However, when we apply both the parity and time reversal operators, the Hamiltonian is preserved; $\mathcal{PT}: H = p^2 + x^2 - (-i)x^3 = p^2 + x^2 + ix^3$.

Let us now consider a standard Hamiltonian of the form $H = \frac{p^2}{2m} + V(x)$. Applying the $\mathcal{PT}$ operator before and after the Hamiltonian, we get $\mathcal{PT}H = \frac{p^2}{2m} + V^*(-x)$ and $H\mathcal{PT} = \frac{p^2}{2m} + V(x)$. So for the Hamiltonian to be $\mathcal{PT}$ symmetric, $V(x) = V^*(-x)$. In other words, for $\mathcal{PT}$ symmetry to hold, the real part of $V(x)$ must be an even function of x, while the imaginary part of $V(x)$ must be an odd function, i.e. the Hamiltonian must have the form $H = \frac{p^2}{2m} + V_R(x) + i\epsilon V_I(x)$, where $V_R(x)$ and $V_I(x)$ are the symmetric and anti-symmetric components of $V(x)$ respectively. Clearly if $\epsilon = 0$ the Hamiltonian is Hermitian, and as Bender et al have shown, the Hamiltonian has entirely spectra when $\epsilon > 0$ but below some threshold value ϵ_{th}. When $\epsilon > \epsilon_{th}$, the spectrum ceases to be real and starts to involve imaginary eigenvalues. This signifies the onset of $\mathcal{PT}$ symmetry breaking and constitutes a "phase transition" from the exact to broken-$\mathcal{PT}$ phase.

2. Applying $\mathcal{PT}$ symmetry theory to optics: A waveguide approach

In optics, several physical processes obey equations that are formally equivalent to Schrodinger's equation, such as spatial diffraction and temporal dispersion. When we look at the spatial domain, in optics, a complex refractive index distribution plays the role of an optical potential. Hence, such $\mathcal{PT}$ symmetric optical potentials can be realized by employing index guiding and gain/loss regions. Given that the refractive index $n(x) = n_R(x) + in_I(x)$, we can design a $\mathcal{PT}$ symmetric system by satisfying $n_R(x) = n_R(-x)$ and $n_I(x) = -n_I(-x)$. Under these conditions, the electric-field envelope E of the optical beam is governed by the equation of diffraction

$$i\frac{\partial E}{\partial z} + \frac{1}{2k}\frac{\partial^2 E}{\partial x^2} + k_0[n_R(x) + in_I(x)]E = 0$$

where $k_0 = \frac{2\pi}{\lambda}, k = k_0 n_0, \lambda$ is the free-space wavelength and n_0 is the substrate index. As an initial study to properly understand $\mathcal{PT}$ behavior, we can study a single-cell optical potential. In integrated optics, the single cell would be a standard coupled system composed of two parallel channels, with one channel being optically pumped to provide gain γ_G, while the neighbor channel experiences loss γ_L [2]. By using the coupled-mode approach, we can formulate the dynamics of the optical fields in the two coupled waveguides as shown below,

$$i\frac{dE_1}{dz} - i\frac{\gamma_{\text{Geff}}}{2}E_1 + \kappa E_2 = 0, \qquad i\frac{dE_2}{dz} - i\frac{\gamma_{\text{L}}}{2}E_2 + \kappa E_1 = 0$$

where $E_{1,2}$ represent the field amplitudes in channels 1 and 2, $\kappa = \frac{2\pi}{L_c}$ is the coupling constant with coupling length L_C and the effective gain coefficient is $\gamma_{\text{Geff}} = \gamma_{\text{G}} - \gamma_{\text{L}}$. $\mathcal{PT}$ symmetry requires that $\gamma_{\text{Geff}} = \gamma_{\text{L}} = \gamma$. We can study the supermodes of the channels both below and above threshold to understand their operation. Below threshold, the modes are given by $|1,2\rangle = (1, \pm\exp(\pm i\theta))$, with corresponding eigenvalues being cos⍰, where $\sin\theta = {}^{\gamma}/_{2\kappa}$. At the phase transition point, the modes become $|1,2\rangle = (1, i)$, where the two channels have the same magnitude. However, above threshold, i.e. for $\gamma > 2\kappa$, $|1,2\rangle = (1, i\exp(\mp i\theta))$, where in this range $\cosh\theta = {}^{\gamma}/_{2\kappa}$ and the two eigenvalues are $\mp i\sinh\theta$. Unlike Hermitian systems, these modes are not orthogonal. Due to this skewed basis, we can observe interesting optical beam dynamics, including non-reciprocal responses and power oscillations. Ruter et al. very theoretically demonstrated this, as shown in Fig 1 below [2].

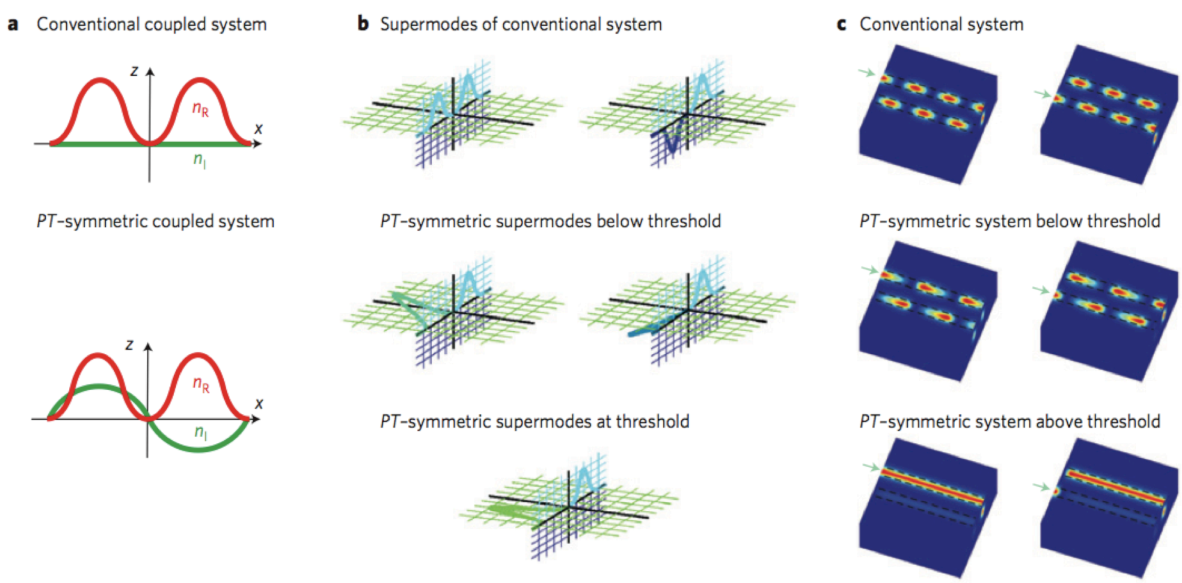

Fig 1. **(a)** Refractive index profile for conventional and $\mathcal{PT}$ symmetric coupled system, **(b)** Supermodes for a conventional system and $\mathcal{PT}$ symmetric systems below and at threshold, **(c)** Optical wave propagation for a conventional system and $\mathcal{PT}$ symmetric systems below and above threshold.

As can be seen in Fig 1c, for a conventional system (top), as expected, we observe reciprocal behavior with relative phase difference of π between the two field components. This changes drastically when the system involves a gain/loss dipole. When we study a $\mathcal{PT}$ symmetric system below threshold (middle), the relative phase difference between the two

field components decreases to $\frac{\pi}{2}$ and the system starts to exhibit non-reciprocal behavior. However, we clearly observe non-reciprocal behavior for the $\mathcal{PT}$ symmetric system above threshold (top). In this regime, light always leaves from channel 1, irrespective of the input channel. This can be explained by the supermodes of the channels – since one has a real mode (exponentially increasing), while the other is imaginary (exponentially decreasing), only one channel effectively survives. Ruter et al proceed to experimentally demonstrate this non-reciprocal behavior by studying waveguides based on Fe-doped $LiNbO_3$. Using Ti in-diffusion to form the symmetric index profile, they provide optical gain through two-wave mixing using Fe-doped $LiNbO_3$'s photorefractive nonlinearity.

3. Applying $\mathcal{PT}$ symmetry theory to optics: A resonator approach

While Ruter et al studied $\mathcal{PT}$ symmetry in a coupled waveguide system, Peng et al conducted a similar study on a resonator-based system [3]. Their $\mathcal{PT}$ symmetric system, as shown below in Fig 1a, was composed of two whispering-gallery microcavities (WGMs), each coupled to a different fiber-taper coupler. The first microtoroid (μR_1) was an active resonator made from Er^{3+}-doped silica, while the second one (μR_2) was a passive resonator made of silica without dopants. Peng et al input a pump beam at 1460nm at Port 1 to provide gain for uR_1 as well as a weak probe signal at 1550nm at Port 1. The microcavities were designed to ensure there was no coupling at 1460nm, hence ensuring that only μR_1 is optically pumped. The output was measured at Port 4. Compensation of the μR_1 losses in the 1550nm band with Er^{3+} was confirmed by the narrowing of the resonance linewidth with increasing peak power, as shown in Fig 1e and by the emergence of a strong resonance peak due to amplification of a very weak probe by the gain.

There is one key difference between this study and Ruter et al's waveguide study in how they shift from exact $\mathcal{PT}$ symmetry to $\mathcal{PT}$ symmetry breaking. While Ruter et al varied the gain in one channel in order to observe this effect, Peng et al controlled the coupling constant between the microtoroids – they fabricated the microtoroids at the edge of two separate chips placed on nanopositioning systems to control precisely the distance and hence the coupling between the microtoroids. Hence, below a certain coupling threshold κ_{th} the system is in a broken-symmetry phase.

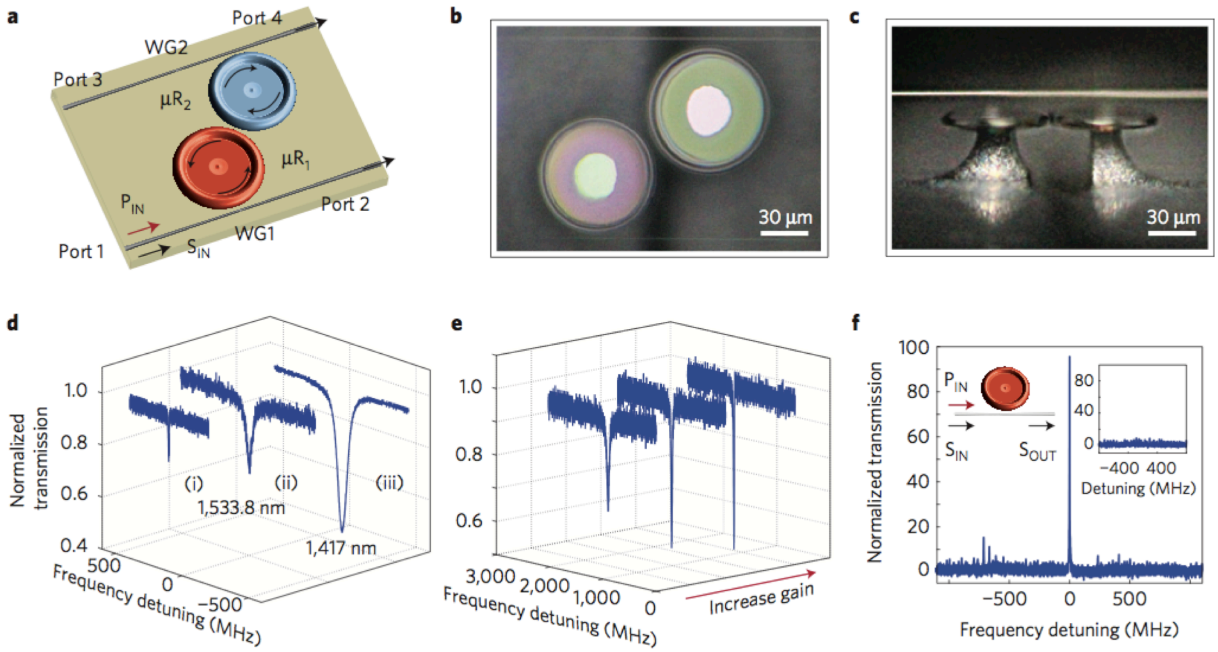

Fig 2. (a) Schematic of system consisting of coupled whispering-gallery microcavities and two fiber-taper waveguides. **(b),(c)** Top and side views of microcavities. **(d)** Transmission spectra showing resonance of μR_2 at 1533.8nm (i) and resonances of μR_1 at 1533.8nm (ii) and 1417nm (iii). **(e)** Gain provided by Er^{3+} ions in μR_1 leads to narrower and deeper resonances as pump power is raised, implying an increasing Q-factor. **(f)** Weak probe beam is amplified when coupled to μR_1 together with the pump light. Inset shows that without the weak S_{IN} there is no resonance enhancement.

Approaching $\mathcal{PT}$ symmetry from a coupling standpoint, Peng et al provide this intuitive picture. If the coupling between the resonators is weak, the energy in the active resonator cannot flow fast enough into the passive resonator to compensate the absorption. Hence the system cannot be in equilibrium and the eigenfrequencies are complex. However if the coupling exceeds a critical value κ_{th} then the system can attain equilibrium because the energy in the active resonator can flow rapidly enough into the passive one.

Peng et al proceeded to study non-reciprocity of light in their system: they make a claim that $\mathcal{PT}$ symmetry alone is not sufficient to achieve non-reciprocity, but nonlinearities enhanced by $\mathcal{PT}$ symmetry breaking are required. They studied this by measuring the output from Port 4 for both the unbroken (linear) phase and symmetry-broken (nonlinear) phase. At low powers (Fig 3a) where input-output relation is linear, they observe reciprocal behavior for both broken and unbroken symmetry phases (Fig 3b,c). However with higher powers and enhanced nonlinearities because of the lower threshold for nonlinearity due to $\mathcal{PT}$ symmetry breaking, they observe non-reciprocity. The also observe unidirectional transmission, as shown in Fig 4.

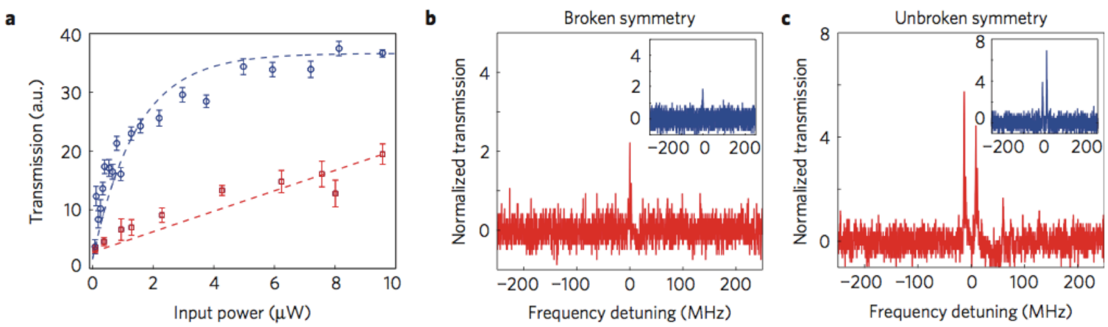

Fig. 3 (a) Linear input–output relation in the unbroken-symmetry region (red square symbols) but nonlinear in the broken-symmetry region (blue circle symbols). **(b)**,**(c)** Transmission spectra in the linear regime (input power of ~80 nW) show reciprocal light transmission at forward (blue inset) and backward (red spectra) directions in both the broken- (**b**) and unbroken- (**c**) symmetry regions. The red (blue) spectra were normalized with the signal detected at port 3 (2) when the input was at port 4 (1) and there was no coupling between the fibre tapers and the resonators.

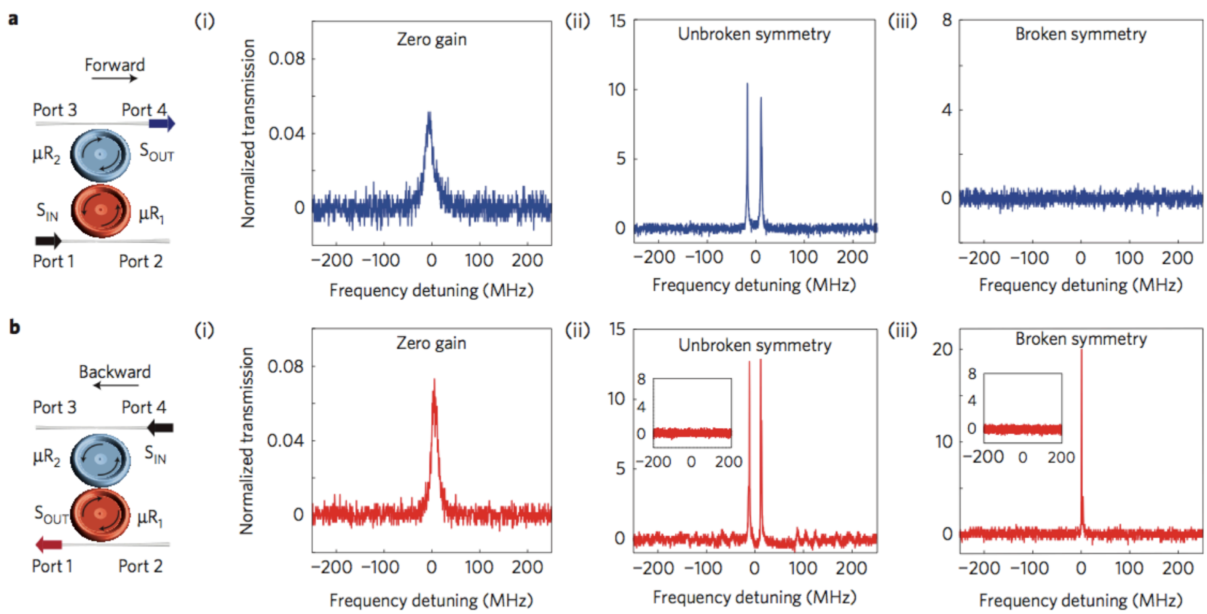

Fig. 4 (a),(b) (left) Schematic for forward (a) and backward (b) transmission. **(a(i),b(i))** Graph shows reciprocal transmission for forward and backward transmission. **(a(ii),b(ii))** Transmission in unbroken symmetry phase is reciprocal. **(a(iii),b(iii))** Transmission is non-reciprocal for broken symmetry phase.

As shown in Fig 4, when both resonators are passive (zero gain), the transmission is bi-directional (reciprocal), and light is transmitted in both forward (a(i)) and backward directions (b(i)). In the unbroken-symmetry region, where the coupling exceeds the critical value and gain and loss are balanced, the transmission is still bi-directional (a(ii),b(ii)). Mode splitting due to coupling is now resolved because gain compensates loss leading to narrower linewidths. In the broken-symmetry region (a(iii),b(iii)), transmission becomes

unidirectional (non-reciprocal). Input in the backward direction reaches the output (b(iii)), but input in the forward direction does not (a(iii)). This resembles the action of a diode and implies that an all-optical on-chip diode with PT-symmetric WGM microcavities operates in the broken-symmetry region. Inset in (b(ii),b(iii)) shows the signal at port 1 when there is no input signal at port 4.

Peng et al admit that this system is bandwidth-limited, but can be expanded to broader bandwidths by using resonators doped with multiple rare-earth ions. Furthermore, by fabricating resonator structures that exhibit sharper Fano resonances, ultralow-power and high-contrast switching and non-reciprocity should be achievable.

4. Conclusions

We have given a brief overview of $\mathcal{PT}$ symmetry, from the theoretical development for optical systems, to demonstration of non-reciprocity of such symmetric systems at the "phase transition" between unbroken and broken symmetry. By designing systems that can switch between these symmetry phases, we can achieve much sharper switching contrast at much lower powers. These systems can also be used to one-way transmission, acting like a diode, one-way invisibility and double refraction [4], among others. These phenomena, while unattainable before, are now within experimental reach and can be further optimized for device-oriented applications.

References:

[1] C.M Bender et al, “Real spectra in non-Hermitian Hamitonians having *PT* symmetry,” *Phys. Rev. Lett.* **80**, 5243-5246 (1998)

[2] K.G. Makris et al, “Beam Dynamics in *PT* Symmetric Optical Lattics,” *Phys. Rev. Lett.* **100**, 103904 (2008)

[3] C.E. Ruter et al, “Observation of parity-time symmetry in optics,” *Nature*. **6**, 192 (2010)

[4] Z. Lin et al, “Unidirectional Inivisibility Induced by *PT*-symmetric Periodic Structures,” *Phys. Rev. Lett.* **106**, 213901 (2011)